Geranylgeranylation Facilitates TNF-α mediated MCP-1 Expression and Release by Rat Peripheral Nerve Microvascular Endothelial Cells

K.A. Langert,[1,2] C.L. Von Zee,[1,3] and E.B. Stubbs, Jr.[1,3]

[1]Research Service, Edward Hines Jr. VA Hospital, Hines, IL; [2]Program of Neuroscience, [3]Ophthalmology, Loyola University of Chicago, Maywood, IL

INTRODUCTION

Guillain-Barré syndrome (GBS) is a leading cause of autoimmune neuromuscular paralysis. Proinflammatory cytokines, particularly TNF-α, play a pivotal role in the pathogenesis of GBS.[1] TNF-α, acting through NF-κB, induces the transcription of many inflammatory mediators, including chemokines. These chemotactic cytokines facilitate the transendothelial migration of autoreactive leukocytes into the sciatic nerve,[2] which is a hallmark feature of the pathogenesis of GBS.[3]

Inhibition of HMG-CoA reductase with statins has been shown to markedly attenuate the course of experimental autoimmune neuritis (EAN), [4] an established animal model of GBS. *In vivo*, statins restrict transendothelial migration of autoreactive leukocytes into peripheral nerves.[4] The mechanism by which this occurs remains unknown, but may involve limiting production of key downstream metabolic intermediates of cholesterol biosynthesis, including the isoprenoids farnesyl pyrophosphate (FPP) and geranylgeranyl pyrophosphate (GGPP). Isoprenylation is a required step in the functional activation of small GTP-binding proteins, including Rho.[5] Activation of RhoA in particular has been shown to regulate cytokine-mediated upregulation of the chemokine monocyte chemoattractant protein-1 (MCP-1), a mediator of leukocyte recruitment that is implicated in the onset and progression on GBS.[6, 7]

In this study, we sought to determine the mechanism by which statins disrupt transendothelial migration using SV40-transformed peripheral nerve microvascular endothelial cells (PNMECs).

METHODS

PNMEC Cell Culture: Rat primary PNMECs were purified from sciatic nerves of naïve male Lewis rats and cultured in Ham's F10 media supplemented with 10% FBS, 100 U/ml penicillin and 0.1 mg/ml streptomycin, 50 µg/ml endothelial cell growth supplement, and 0.1% heparin at 37°C under an atmosphere of 5% CO_2/95% air. Primary PNMECs were immortalized by SV40 transduction using an SVU19.5 producer cell line expressing a replication deficient SV40 retrovirus with a neomycin resistant gene (Dr. P. Jat, University College of London, London, UK). Following transduction, PNMECs were plated into complete culture media containing G418 (200 µg/ml). G418-resistant cell lines were isolated by single colony selection. A single clone (4.3) demonstrating morphological and immunocytochemical characteristics of primary PNMEC cultures was expanded and analyzed.

Treatments: Confluent cultures were treated with media alone (vehicle control) or with TNF-α as indicated. In some cases, cultures were pretreated (1-16h, as indicated) with vehicle (0.01% ethanol or 0.5% DMSO), lovastatin, simvastatin, or pravastatin, with a direct inhibitor of geranylgeranyl transferase-1 (GGTI-298) or farnesyl transferase (FTI-277), or with selective GTPase inhibitors (NSC23766, ML141, or C3 exoenzyme) as specified.

Immunocytochemistry: Cells were cultured on collagen-coated coverslips, fixed, blocked, and incubated overnight at 4°C in the presence of mouse anti-Von Willebrand factor (VWF, 1:50 dilution), mouse anti-PECAM-1 (CD31, 1:100 dilution), or rabbit anti-MCP-1 (1:200 dilution) primary antibody. Immunostained cells were incubated for 1h at 23 C in the presence of AlexaFluor-488 conjugated goat anti-mouse secondary antibody (1:1000 dilution) or FITC-conjugated goat anti-rabbit secondary antibody (1:100 dilution), respectively, and counterstained with DAPI.

Real Time RT-PCR: Total RNA was extracted from treated cultures with TRIzol reagent and 5.0 µg reverse transcribed using Super Script III First-Strand Synthesis system. MCP-1 and GAPDH specific cDNA sequences were amplified by real-time (iQ SYBR Green) quantitative RT-PCR using a Mini-Opticon PCR detection system with published rat-specific primer pairs. GAPDH was used as a reference control. For each sample, the specificity of the product was determined by melt-curve analysis. The endogenous expression of GAPDH was unaltered by drug treatment. Relative fold-changes in MCP-1 mRNA content were normalized to expressed levels of GAPDH using the $2^{-\Delta\Delta CT}$ method of Livak.

MCP-1 ELISA: Cells were cultured on collagen-coated 24- or 96-well plates, treated as indicated, and fixed with buffered (pH 7.4) 4% PFA. For whole-cell MCP-1 analysis, fixed cells were incubated overnight at 4 C in the presence of rabbit anti-MCP-1 (1:200 dilution) primary antibody as indicated. Immunostained cells were washed and incubated for 1h at 23 C in the presence of HRP-conjugated goat anti-rabbit (1:10,000 dilution) secondary antibody. MCP-1 content was determined colorimetrically (OPD) at 492 nm. Specific content was expressed as percent increase over unstimulated control cells. For quantifying secreted MCP-1, culture medium from treated cells were collected and stored at -80°C until use. The content of MCP-1 released into the culture media was quantified using a commercially available ELISA kit (Thermo Scientific).

Transendothelial migration assay: The upper chamber of a 24-well Transwell plate was seeded with 10^5 transformed PNMECs to establish an endothelial monolayer. After two days in culture, THP-1 monocytic cells (10^5) were added to the upper chamber and migration initiated by placing the upper chamber into conditioned media (0.6 ml) harvested from TNF-α treated (4h, 10ng/ml) PNMECs that were pretreated with vehicle (0.6% DMSO) or GGTI-298 (10 µM). In a separate experiment, conditioned media was incubated with a function-blocking antibody to MCP-1 prior to migration. After 4h, cells that had migrated into the lower chamber were collected and counted with a hemocytometer.

RESULTS

Figure 1. Characterization of SV40-transformed PNMECs

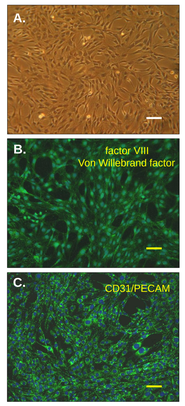

Representative **(A)** phase contrast and **(B,C)** immunofluorescent images of immortalized PNMECs (bar, 50 µm). **(D)** Immunoblot of Large T antigen protein expression in whole-cell lysates prepared from primary PNMECs and transformed (clone 4.3) PNMECs, as indicated.

Figure 2. TNF-α increases MCP-1 mRNA and protein

MCP-1 mRNA (GAPDH-normalized fold change)		
	Vehicle	TNF-α (10 ng/ml, 3h)
Primary PNMECs	1.00 ± 0.16	12.66 ± 5.16*
Immortalized PNMECs	1.00 ± 0.12	44.93 ± 4.27*
MCP-1 intracellular protein (percent change from quiescent)		
	Vehicle	TNF-α (10 ng/ml, 3h)
Primary PNMECs	n.a.	n.a.
Immortalized PNMECs	0.00 ± 2.05	66.07± 4.25*
MCP-1 protein secretion (ng/ml)		
	Vehicle	TNF-α (10 ng/ml, 4h)
Primary PNMECs	7.56 ± 0.43	36.01 ± 1.56*
Immortalized PNMECs	38.62 ± 8.14	194.9 ± 25.53*

Summary of RT-PCR, cell-based ELISA, or standard ELISA analysis of MCP-1 expression in the absence (Vehicle, media) or presence (3-4h, 10 ng/ml) of TNF-α. Data shown are the means ± SEM (N=6-12) of at least two separate experiments. n.a., not analyzed; *, p<0.05; Student's t-test.

Figure 3. Inhibition of protein prenylation does not alter TNF-α mediated increases in mRNA content

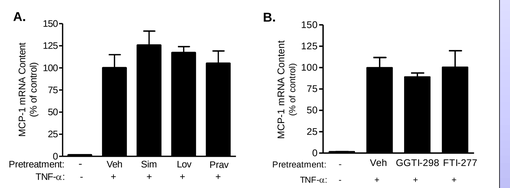

Effect of **(A)** vehicle (Veh, 0.01% ethanol), simvastatin (Sim), lovastatin (Lov), or pravastatin (Prav) or **(B)** vehicle (Veh, 0.6% DMSO), GGTI-298 or FTI-277 pretreatment (10 µM, 16h) on TNF-α (4h, 10 ng/ml) mediated increases in MCP-1 mRNA content. GAPDH-normalized data are shown as the percent change from vehicle-pretreated TNF-α control from two separate experiments (N=3-9), expressed as mean ± SEM.

Figure 4. Inhibition of protein prenylation does not alter TNF-α mediated increases in intracellular MCP-1 protein expression

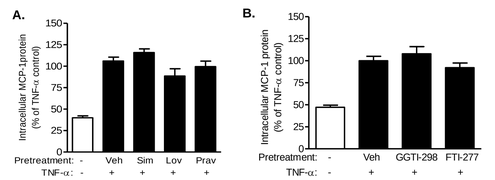

Effect of **(A)** vehicle (Veh, 0.01% ethanol), simvastatin (Sim), lovastatin (Lov), or pravastatin (Prav) or **(B)** vehicle (Veh, 0.6% DMSO), GGTI-298 or FTI-277 pretreatment (10 µM, 16h) on TNF-α (4h, 10 ng/ml) mediated increases in MCP-1 protein content, as quantified by cell-based ELISA. Data shown are percent change from vehicle-pretreated TNF-α control from two separate experiments (N=8), expressed as mean ± SEM.

Figure 5. Simvastatin attenuates TNF-α mediated increases in MCP-1 protein secretion

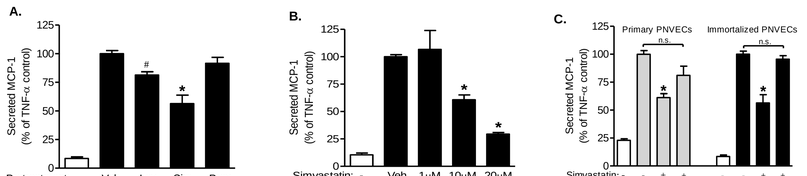

Effect of overnight pretreatment with vehicle (veh, 0.01% ethanol), lovastatin (Lov, 10 µM), simvastatin (Sim, 1-20 µM, ± 10 µM GGPP), or pravastatin (Prav, 10 µM), on TNF-α (10 ng/ml, 4h) mediated secretion of MCP-1 protein. Data shown are the means ± SEM (N=3-6). *, p<0.01; #,p<0.05 compared with vehicle pretreated TNF-α control; one-way ANOVA with Bonferroni's post-hoc analysis.

Figure 6. Inhibition of geranylgeranylation attenuates TNF-α mediated increases in MCP-1 protein secretion

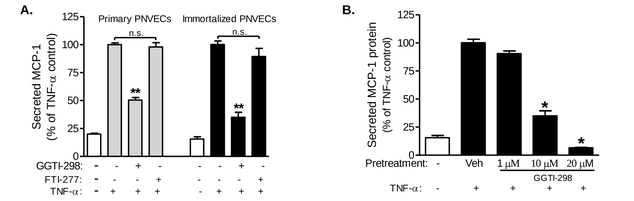

Effect of pretreatment with vehicle (0.6% DMSO) or direct inhibitors of geranylgeranylation (GGTI-298, 0-20 µM) or farnesylation (FTI-277, 10 µM) on TNF-α (10 ng/ml, 4h) mediated secretion of MCP-1 protein. Data shown are the means ± SEM (N=3-6). *, p<0.05; **,p<0.01 compared with vehicle pretreated TNF-α control; one-way ANOVA with Bonferroni's post-hoc analysis.

Figure 7. Disruption of geranylgeranylation attenuates transendothelial migration

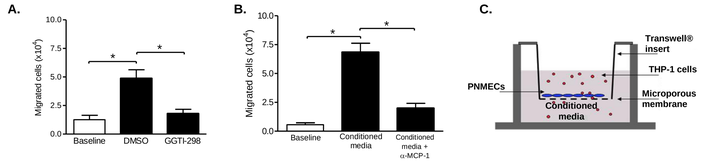

PNMECs were pretreated overnight without (DMSO, 0.6%) or with GGTI-298 (10 µM) **(A)** followed by incubation with TNF-α (10 ng/ml, 4h). Conditioned media containing MCP-1 (± an MCP-1 neutralizing antibody, **B**) was transferred to the lower chamber of a Transwell plate (depicted in **C**). Monocytes migrated (4h) into conditioned media across a monolayer of PNMECs (see **C**). Migrated cells were counted with a hemocytometer. Data shown are the means ± SEM (N=6). *, p<0.01; one-way ANOVA with Bonferroni's post-hoc analysis.

Figure 8. GGTI-298 disrupts intracellular MCP-1 protein distribution in PNMECs

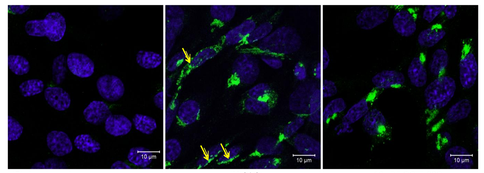

Effect of GGTI-298 pretreatment (10 µM, 16h) on TNF-α (10 ng/ml, 4h) mediated expression and distribution of intracellular MCP-1 protein. Arrows indicate punctate, vesicle-like structures.

Figure 9. Cdc42 facilitates TNF-α mediated increases in MCP-1 protein secretion

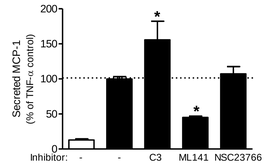

Effect of pretreatment with selective GTPase inhibitors on TNF-α (10 ng/ml, 4h) mediated secretion of MCP-1 protein. Data shown are the means ± SEM (N=3-6 cultures); *, p< 0.01 versus vehicle pretreated TNF-α control; one-way ANOVA with Bonferroni's post-hoc analysis.

SUMMARY/CONCLUSION

- SV40-transformed rat peripheral nerve microvascular endothelial cells retain a phenotype characteristic of primary endothelial cells
- TNF-α elicits marked increases in MCP-1 mRNA and protein expression and protein secretion and induces MCP-1 dependent transendothelial migration of THP-1 monocytes *in vitro*
- Inhibition of protein geranylgeranylation attenuates TNF-α mediated increases in secreted MCP-1 protein, as well as chemotaxis of THP-1 monocytes, independently of mRNA or intracellular protein expression
- Intracellular trafficking and vesicle release of MCP-1 is dependent , in part, on Cdc42 GTPases

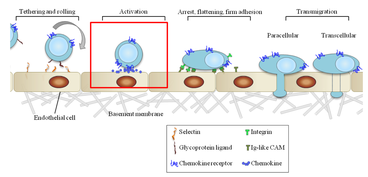

TNF-α dependent enhancement of MCP-1 protein release from peripheral nerve microvascular endothelial cells occurs by a mechanism that involves, in part, post-translational geranylgeranylation of Cdc42

Attenuation of endothelial cell MCP-1 expression may be of therapeutic value in the management of inflammatory autoimmune disorders

REFERENCES

1. Zhu J, *et al*. Cytokine production and the pathogenesis of experimental autoimmune neuritis and Guillain-Barré syndrome. *J Neuroimmunol*. 1998; 84, 40-52.
2. Springer T. Traffic signals for lymphocyte recirculation and leukocyte emigration: The multistep paradigm. *Cell*. 1994; 76:301-314.
3. Hartung H, *et al*. Immunopathogenesis and treatment of the Guillain-Barré Syndrome- Part I. *Muscle & Nerve*. 1995; 18:137-153.
4. Sarkey J, *et al*. Lovastatin attenuates nerve injury in an animal model of Guillain-Barré Syndrome. *J Neurochem.* 2007; 100:1265-1277.
5. Zhang F & Casey P. Protein prenylation: mechanisms and functional consequences. *Ann Rev Biochem* 1996; 65:241-269.
6. Greenwood J & Mason J. Statins and the vascular endothelial inflammatory response. *Trends Immunol.* 2007; 28:88-97.
7. Orlikowski D, *et al*. MCP-1 and CCR2 productions in Guillain-Barré syndrome and experimental autoimmune neuritis. *J Neuroimmunol*. 2003; 134:118-127.

ACKNOWLEDGEMENTS:

This work was supported, in part, by grants from the Department of Veterans Affairs (B3413R, B3756F), NIH (1R03NS061033), and a VA Pre-Doctoral Associated Health Rehabilitation Research Fellowship (KAL).